A Summary of the Theory of Velocity Selective Neural Recording

John Taylor, Martin Schuettler, Chris Clarke and Nick Donaldson

***Abstract*—This paper describes improvements to the technique of *velocity selective recording* (VSR) in which multiple neural signals are matched and summed to identify excited axon populations in terms of velocity. This form of recording has been termed *intrinsic velocity selective recording* (IVSR). The signals are acquired using a multi-electrode cuff (MEC) which is now available as a component for use in implantable neuroprostheses. The improvements outlined in the paper involve the use of bandpass filters at the output of the system which allows a higher level of selectivity to be obtained than is possible using IVSR.**

I. Introduction

Velocity selective recording (VSR) is a technique which should allow more information to be extracted from an intact nerve with a recording set-up that does not allow action potentials from single fibres to be seen at spikes [1]-[3]. The method is in essence very simple and relies on taking measurements of a propagating *action potential* (AP) at two or more points. The distance between the sample points divided by the delay between the appearance of the two replicas of the AP provides a measure of the propagation velocity. Perhaps unsurprisingly, this very simple idea is not new and various researchers have investigated practical adaptations of it in the past (*e.g.* [6]-[8]).

However, at present the idea has not been demonstrated with naturally-occurring nerve traffic though experimenters have used *multi-electrode cuffs* (MECs) to observe appropriate outputs from compound action potentials [3]-[5]. The authors have published two papers about the theory of VSR [1]-[2]. The first presented a spectral analysis of a single axon in an MEC with a *tripolar* (double-differential) amplifier system and the signal processing arrangement shown in Figure 1. The bandpass filter (BPF) that follows the adder was shown to improve selectivity in the *velocity domain*. The second paper [2] considered the thermal noise generated by the detection system and compared its amplitude to that of the signal resulting from the summation of multiple *single fibre action potentials* (SFAPs) which were assumed to occur at random times. This allows the calculation of the firing rates required from various sizes of nerve fibre in a given MEC to provide a signal that could be detected above the background noise.

The current paper presents material which supplements and expands the earlier work described in refs [1] and [2]. In essence it is a study (by simulation) of improvements in velocity selectivity obtainable by the use of BPFs, investigating in particular the limitations of the method with and without additive noise. Preliminary measured data in *pigs* is also presented.

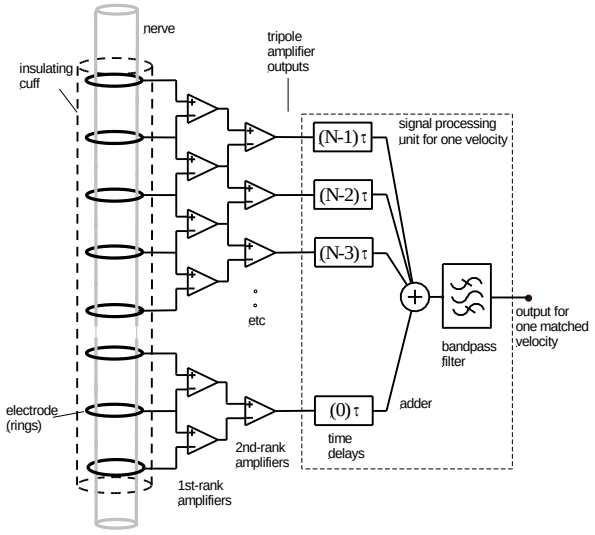

Figure 1. This shows a *multielectrode cuff* (MEC) connected to a *tripolar* (double differential) amplifier array. The *N* tripolar outputs (where *N* is typically about 10) are digitised and processed in the signal processing unit on the right of the figure.

II. Background

A. Basic principles

The input to the MEC is a *trans-membrane action potential* function (TMAP), $V_m(t)$, with the corresponding spectrum $V_m(f)$. The resulting SFAP is a propagating wave with the time dependence of the underlying TMAP function, the relationship between the two being explained in [1]. We represent the TMAP function and its spectrum by the following Fourier transform pair [1]:

$$V_m(t) = At^n e^{-Bt}$$

$$V_m(f) = \frac{n!A}{(B + j2\pi f)^{n+1}} \qquad \ldots (1)$$

where A, B and n are constants and f is frequency (the symbology has been preserved from [1]). The output $Y(f, v)$, which is a function of both frequency and velocity, is obtained by treating the MEC as a linear time-invariant system with transfer function $H(f, v)$ [1]. At *matched*

Manuscript received March 26, 2011. This work was supported in part by the Engineering and Physical Sciences Research Council (EPSRC) UK and by the German Academic Exchange Service (DAAD).

John Taylor (corresponding author +44 1225 38 3910) and Chris Clarke are with the Department of Electronic and Electrical Engineering, University of Bath, Bath BA2 7AY UK.

Martin Schuettler is with the Laboratory for Biomedical Microtechnology, Department of Microsystems Engineering – IMTEK, University of Freiburg, 79110 Freiburg, Germany.

Nick Donaldson is with the Department Medical Physics and Bioengineering, University College London, London WC1 UK.

velocities (i.e. where the inserted delay $\tau = d/v$ and $v = v_o$), *Y(f, v)*, reduces to:

$$Y(f, v_0) = 4N \frac{R_e}{R_a} \sin^2\left(\frac{\pi f d}{v_0}\right) \cdot \left| \frac{A}{(B + j2\pi f)^2} \right| \quad \ldots (2)$$

where R_a and R_e are the intra- and extra-axonal resistances per unit length, respectively. The output of the system *Y(f,v)* is a function of two variables and it was pointed out in [1] that if *f* is fixed by passing the output through a bandpass filter (so that $f = f_0$), *Y* becomes a function of propagation velocity *v* only, enabling the *velocity selectivity* profile (see the *tuning curves* in [1]) to be calculated readily.

We define a *velocity quality factor*, Q_v, by analogy with linear systems in the frequency domain [2]:

$$Q_v = \frac{v_0}{v_{3+} - v_{3-}} \quad \ldots (3)$$

where v_0 is the matched (i.e. peak) velocity and v_{3+} and v_{3-} are the velocities at which the output has fallen to $1/\sqrt{2}$ (-3 dB) of the peak value. Close to the matched velocities, the velocity selectivity is dominated by the function *G(f,v)* and in [2] an approximate formula for Q_v was derived:

$$Q_v \cong \frac{N\pi d f_0}{2.64 v_0} \quad \ldots (4)$$

B. The intrinsic velocity spectrum (IVS)

If filtering is not applied, the output will depend on *v* and on frequency dependent elements in the system including the spectral properties of the input signal (i.e. the TMAP function) and the characteristics of the channel. For these reasons, unlike the bandpass filtered version, the *intrinsic velocity spectrum* (IVS) is quite difficult to interpret.

Table 1
TMAP Parameters ($x(t) = At^n e^{-Bt}$)

Parameter	TMAP #1	TMAP #2
A	7.44×10^{11}	4.08×10^3
B	10^4	1.5×10^4
n	3	1

Fig 2 is the time-domain output of the adder in Fig 1 when the system is stimulated with a TMAP resulting in an SFAP propagating at a velocity of 30 m/s. Two TMAP functions are considered, both of which have been proposed as suitable approximations for the simulation of mammalian ENG [9]. The functions are in the form of eqn (1) with the parameters given in Table 1 (the scaling parameter *A* has been adjusted so that the peak amplitudes of the functions are normalised to unity). The matched velocity v_o is treated as a parameter leading to the family of curves shown in the figure. The peak value is reached when the artificial delays exactly match (cancel) the naturally-occurring delays at which point the output signal has the same form as a single SFAP, with amplitude multiplied by *N* [1].

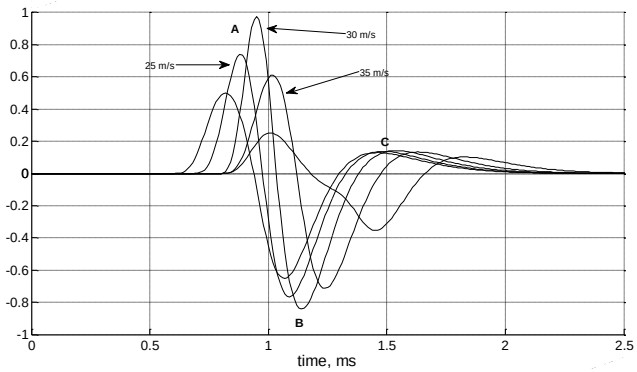

Figure 2. Time domain response of the system shown in Fig 1 (output of the summer), stimulated with TMAP #1 (see Table I) with a propagation velocity of 30 m/s. The three peaks of the waveforms are labelled *A*, *B* & *C*.

Fig 3 shows the IVS of the system, stimulated by an SFAP generated by TMAP#1. This is a plot of the peak values of the output time record (Fig 2) as a function of velocity after the tripole signals have been subjected to delay and add operations *only*. Each curve in the time record shown in Fig 2 has *three* peaks, labelled *A*, *B* and *C*, two positive and one negative, corresponding to the phases of the tripolar SFAP. Whilst it is possible to calculate the IVS at all the peaks, this paper considers only the two larger-amplitude peaks *A* and *B*. The resulting spectra peak at the same matched velocity (40 m/s), but have different selectivities as shown in Fig 3, where the two IVS plots are shown together with the values of Q_v calculated from the figure using eqn (3). These values of intrinsic velocity selectivity are used as baseline references for the enhancements described in the next section.

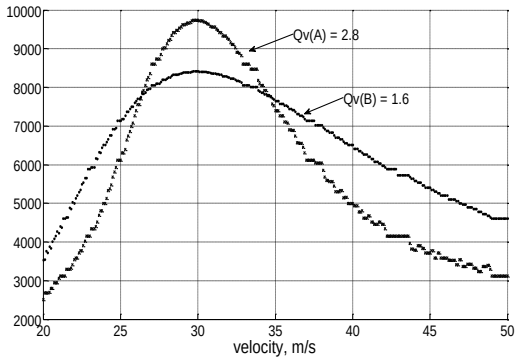

Figure 3. Intrinsic velocity spectra (IVS) for TMAP#1 derived from Fig 2 measured at points A and B.

From the above observations, it is clear that if this method is to be used to separate neural signals in terms of velocity, certain problems of interpretation arise:

1. The measured IVS depends on the point in the time record of the delayed and summed signal used to make the measurement;
2. The IVS profile depends on the properties of the TMAP function, in particular, shorter time records result in larger values of Q_v;

3. The actual selectivity obtainable is quite low and declines with increasing velocity. This accords with the theory presented below (see also ref [2]).

These issues are considered in the next section.

III. Improved Velocity Selective Recording Using Bandpass Filters (BPFVS)

Suppose a BPF is placed at the output of each tripolar amplifier of the VSR system as shown in Fig 1. The effect is to replace each SFAP (which is a tri-phasic pulse in the time domain) with a burst of damped sinewaves whose frequency is the centre frequency of the BPF. The 'delay matching' process is therefore transformed into matching delayed sinewaves rather than complex SFAP waveforms as in the intrinsic case. Unlike the SFAP waveform itself, the BPF output has no dependence on the characteristics of the TMAP except for its amplitude and its exact position in the time record. In addition, since the voltage excursions at the outputs of each BPF are approximately symmetrical (i.e. $\pm V$), there is only one velocity spectrum. It is simply necessary to measure the peak (+ve. or –ve.) of the delayed and summed BPF outputs. The addition of BPFs in this way allows the measurement of velocity selectivity to be decoupled from the spectral properties of the TMAP and to be controlled by means of the centre frequency of the filters which is, at least to some extent, a free parameter.

IV. Simulated and Measured Results

A. Simulated results without noise

In order to demonstrate the effects of adding BPFs to a delay-matched IVS system, the MATLAB simulations shown in Figs 2 and 3 were repeated with a single bandpass filter of centre frequency f_0 placed at the output of the system, as shown in Fig 1 (this is electrically equivalent to placing a filter at the output of each channel due to the linearity of the system). The SFAP was generated using TMAP#1 and the system was noiseless. The filter was an 8^{th}-order digital Butterworth BPF and centre frequencies of 1 kHz, 2 kHz, 4 kHz, 8 kHz or 16 kHz and relative bandwidth 20% were used. The velocity spectra are plotted in Fig 4 and show good responses at the matched velocities. It can be shown that it is possible to obtain satisfactory responses for BPFs with centre frequencies up to the Nyquist frequency (50 kHz in this case). Repeating the simulation using TMAP#2 produces responses that are identical to those shown in Fig 5 in the sense that the values of Q_v measured at the matched velocities are the same in both cases. This supports the assertion that the bandpass filtered velocity selectivity depends only on N, f_0 and v and some physical constants, *not* on the characteristics of the TMAP function, as is the case for IVS. The values of Q_v are listed in Table 2 together with values calculated from eqn (4). The calculated values fit the simulated ones very well.

Table 2
Comparison of Simulated and Calculated Values of Q_v for a 9-Channel Filtered VSR System for a Single SFAP with propagation Velocity 30 m/s

BPF Centre Frequency, f_0 (kHz)	TMAP #1	TMAP #2	Calculated value*
1	0.8	0.8	0.8
2	1.9	1.9	2.0
4	4.3	4.0	4.2
8	7.5	7.5	8.5
16	17.0	16.0	17.1
32	33.3	33.3	34.2

*Calculated using equation (4)

B. Simulated results with additive noise

Zero-mean white Gaussian noise was added to the system in a manner consistent with the approach adopted in [2] (i.e., 11 sources of uncorrelated voltage noise were introduced, one at the input to each *monopolar* channel). These noise sources represent the total noise present in each channel referred to the input. As noted in [2] the total input-referred noise is the sum of several individual sources which are assumed to be independent and uncorrelated.

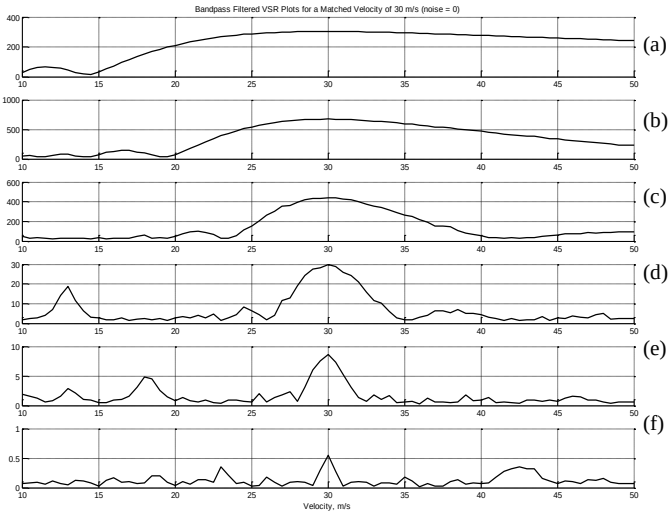

Figure 4. Bandpass filtered version of the IVS plot shown in Fig 2 using TMAP function #1 to generate an SFAP with a propagation velocity of 30 m/s. The filters are 8^{th} order Butterworth digital units with centre frequencies f_0 are (a) 1 kHz, (b) 2 kHz, (c) 4 kHz, (d) 8 kHz, (e) 16 kHz and (f) 32 kHz. The corresponding values of Q_v are 1.4, 2.9, 5.7. The velocity step is 1 m/s and there is no additive noise.

In order to test the effect of the noise on the system and in particular on the ability of the BPFs to increase the velocity selectivity compared to IVS, the simulations described in Section *A.* were repeated with varying levels of additive white Gaussian noise. The results are presented in Table 3 for three values of SNR (1, 10, 100) for each of the two TMAPs. The frequency in column *A* for each value of SNR gives the maximum frequency (f_{omax}) at which an intelligible output is obtainable from a BPF centred at that frequency. Once f_{omax} has been determined, the maximum available velocity selectivity (Q_v) can be calculated from eqn (10) (column *B*) and the enhancement factor found (i.e. compared to IVS-column *C*). In general TMAP#2 performs better than TMAP#1, due to the wider bandwidth of the signal. There is thus more energy at higher frequencies in SFAPs generated from TMAP#2, whilst the additive noise has the same

spectral density at all frequencies and for both TMAPs. In the worst case considered, with SNR set to unity, there is no enhancement in Q_v for TMAP#1, whilst for TMAP#2 a modest enhancement of about 3.5 is possible. For SNR = 10 the values increase to 2 and 7 respectively and 4 and 7 respectively for SNR = 100, although in this case, higher values could be obtained for TMAP#2 if more bandwidth were available.

Table 3
Simulated maximum available velocity selectivity (Q_v) as a function of signal-to-noise ratio for a 9-tripole system. The input is an SFAP propagating at 30 m/s and the limiting resolution is 10-bits

SNR	**1**			**10**			**100**		
	A	*B*	*C*	*A*	*B*	*C*	*A*	*B*	*C*
TMAP#1	4 kHz	2.9	1	8 kHz	5.7	2	16 kHz	12.5	4
TMAP#2	16 kHz	12.5	3.5	32 kHz	25	7	32 kHz	25	7*

Column *A*: maximum available frequency, f_{omax}; column *B*: resulting maximum velocity selectivity; column *C*: velocity selectivity enhancement compared to IVS
*limited by analogue bandwidth (32 kHz)

Finally, in order to provide some preliminary validation of the theory and simulated results presented in this paper, acute *in vivo* recordings were made from the *medial* nerve of a Danish Landrace pig. These experiments were part of a larger study and the detailed description is given elsewhere [10]. The set-up consisted of an 11-electrode MEC (i.e. N = 9) and a tripolar stimulating cuff and the data was captured processed using MATLAB in the same manner as the simulated data reported above. Fig 5 shows the BPFVS for four 8th-order Butterworth digital BPFs with centre frequencies (f_o) 4 kHz, 8 kHz, 10 kHz and 16 kHz. In spite of the fact that the analogue bandwidth of the channels was only about 3.5 kHz, it was still possible to obtain intelligible outputs from all these filters, as the plots in the figure show.

As was the case for the simulated data, measured values of Q_v scale linearly with f_o as predicted by theory (see eqn 4). In addition, as the selectivity is increased, additional velocity peaks become visible. These are indicated by the black arrows in Fig 5 For example, the output at 30 m/s, barely visible in the IVS becomes clear as f_o increases. Furthermore, a signal at about 38 m/s is visible in both the 10 kHz and 16 kHz filter outputs and one at about 42 m/s is visible in the 16 kHz filter output only. These latter signals are completely invisible in the IVS and only appear as the velocity selectivity is increased. Clearly these conclusions are preliminary and speculative and require confirmation from a properly-conducted experimental study.

V. Conclusions

This paper has described a method to improve significantly the performance of velocity selective neural recording (VSR) systems using delay matching by means of bandpass filtering. Simulated results are presented and preliminary validation is provided by some measured data obtained from acute *in vivo* experiments in *pig*.

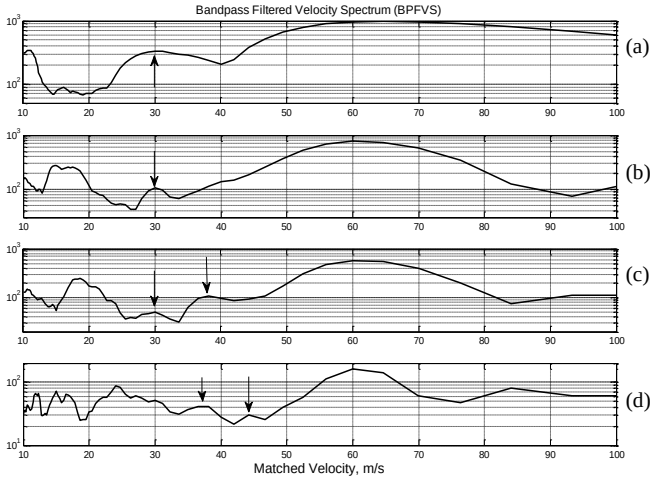

Figure 5. Preliminary measured data from *pig*. The filters are 8th order digital Butterworth units with centre frequencies (f_o) of (a) 4 kHz, (b) 8 kHz, (c) 10 kHz and (d) 16 kHz. The Q_v values of the output corresponding to the fast fibre population (approx 60 m/s) are 1.6, 3.3, 4.6 and 6.5. The output of the population at about 30 m/s is clearly visible. The vertical arrows also indicate the appearance of other populations (e.g, 38 m/s, 44 m/s approx.) as the selectivity is increased. The presence of images can also be noted, at low velocities (i.e. < 30 m/s), dependent on f_o.

References

[1] Taylor J., Donaldson N., & Winter J. (2004) "The use of multiple-electrode nerve cuffs for low velocity and velocity-selective neural recording." *Med. & Biol. Eng. & Comput.*, 42 (5), 634-43.

[2] Donaldson , N., Rieger, R., Schuettler, M. & Taylor, J. (2008) "Noise and Selectivity of Velocity-Selective Multi-Electrode Nerve Cuffs*." Med. & Biol. Eng. & Comput*., 42 (5), 634-43.

[3] Rieger R., Schuettler M., Pal D., Clarke C., Langlois P., Taylor J. & Donaldson N. (2006) "Very low-noise ENG amplifier system using CMOS technology." *IEEE Trans Neural Syst Rehabil Eng.* 14(4):427-37.

[4] Rieger, R., Taylor, J., Comi, E., Donaldson, N., Russold, M., Jarvis, Mahoney, C., & Mclaughlin, J. (2004): "Experimental Determination of Compound A-P Direction and Propagation Velocity from Multi-Electrode Nerve Cuffs." *Medical Engineering & Physics*

[5] Yoshida, K., Kurstjens, G., & Hennings, K. (2009) "Experimental validation of the nerve conduction velocity selective recording technique using a multi-contact cuff electrode." *Medical Engineering & Physics* 31 1261-1270.

[6] Haughland, M. et al (1997) "Restoration of lateral hand grasp using natural sensors." *Artificial Organs* 21 (3) 250-253.

[7] Hoffer J., Loeb G., Pratt C. (1981) "Single Unit Conduction Velocities from Averaged Nerve Cuff Electrode Records in Freely Moving Cats", *Journal of Neuroscience Methods*, Vol. 4, pp.211-225.

[8] Hoffer, J. (1990): "Techniques to study spinal cord, peripheral nerve and muscle activity in freely moving animals." In: *Neuromethods, 15: Neurophysiological Techniques: Applications to Neural Systems*. 65-145, Boulton, A.A., Baker, G.B., Vanderwolf, C.H. (eds), The Humana Press Inc., Clifton, NJ.

[9] Struijk, J. (1997) "The extracellular potential of a myelinated nerve fibre in an unbounded medium and in nerve cuff models." *Biophys. J.*, 72, pp. 2457-2469.

[10] Schuettler, M., Seetohul, V., Rijkhoff., N.J.M., Moeller, F., Donaldson, N., and Taylor, J. (2011): "Fibre-Selective Recording from Peripheral Nerves using a Multiple-Contact Cuff: Report on Pilot Pig Experiments", Proceedings IEEE EMBC.